Glucose and pH Dual-Responsive Nanogels for Efficient Protein Delivery

Xinghui Si, Wantong Song,* Shengcai Yang, Lili Ma, Chenguang Yang, and Zhaohui Tang*

Direct delivery of protein suffers from their in vitro and in vivo instability, immunogenicity, and a relatively short half-life within the body. To overcome these challenges, pH and glucose dual-responsive biodegradable nanogels comprised of dextran and poly(L-glutamic acid)-*g*-methoxy poly-(ethylene glycol)/phenyl boronic acid (PLG-*g*-mPEG/PBA) are designed. The cross-linked network imparted drug-loading efficacy of α-amylase up to 55.6% and hyaluronidase up to 29.1%. In vitro protein release profiles reveal that the release of protein is highly dependent on the pH or glucose concentrations, that is, less amount of protein is released at pH 7.4 or healthy blood glucose level (1 mg mL^{-1} glucose), while quicker release of protein occurs at pH 5.5 or diabetic blood glucose level (above 3 mg mL^{-1} glucose). Circular dichroism spectra show that the secondary structure of released protein is maintained compared to naive protein. Overall, the nanogels have provided a simple and effective strategy to deliver protein.

1. Introduction

Insulin was the first FDA approved recombinant protein 36 years ago, since then the development of protein therapeutics has experienced an explosive growth.[1] Now protein drugs play a vital role for treating a broad range of diseases, including cancer, metabolic disorders, and autoimmune diseases.[2] Certain types of protein drugs like Atezolizumab, zinbryta, and cytochrome C have been approved by FDA for clinical use.[3–6] Protein drugs have been widely applied in the treatment of various diseases attributed to their high specificity, great

activity, and superior biocompatibility.[7,8] Although protein drugs have attracted much attention, there are still many challenges in the application and development. Protein drugs can easily be denatured by temperature, pH, organic solvent, and so on.[9,10] Therefore, direct usage of protein drugs suffers from instability, immunogenicity, and short blood circulation. Protein drugs have poor membrane penetration ability, which limits their usage for arriving at intracellular targets.[11–14] More importantly, controllable release of protein drugs is difficult to achieve. Therefore, vast efforts have been exploited for protein drug delivery. Wu et al. have developed PLGA-polycation (PC) nanoparticles by conjugating L-arginine-based polycation to the diblock copolymer of poly(lac-tide-*co*-glycolic acid) (PLGA). BSA, insulin, and TNF-α, three kinds of negatively charged proteins, were captured by the nanoparticles without organic solvent though electrostatic interactions. The complex nanostructure performed more than 20 wt% of protein-loading capacity, and achieved sustained release for several weeks. This simple and green strategy has offered new platforms for protein delivery.[15]

Nanogels, innovative, and versatile carriers combining the advantages of nanoparticles and hydrogels have attracted considerable attention in drug delivery.[16] Nanogels have nano-sized aqueous crosslinked polymer networks and, like hydrogels, possess excellent biocompatibility and high loading capacities for therapeutics.[17–20] For these distinctive advantages, nanogels have been applied widely for drug delivery, especially protein drugs which easily deactivate and break down. Lu et al. designed an intracellular delivery platform for protein delivery. The nanogels were consisted of a single-protein core and thin polymer shell anchored covalently to the protein core. A vast library of proteins including caspase-3, enhanced green fluorescent protein, and bovine serum albumin can be chosen as the cores. Then, polymerizable vinyl groups were covalently linked to caspase-3, a family of cysteine proteases that play essential roles in apoptosis, necrosis, and inflammation. Subsequently, the protein was copolymerized with acrylamide, 2-dimethylaminoethyl methacrylate, and an acid cleavable glycerol dimethacrylate crosslinker for the caspase-3-nanogels. After caspase-3-nanogels were internalized into HeLa cells, the nanogels broken down in the acidic conditions and caspase-3 was released from the nanogels. The caspase-3 nanogels showed significantly higher cytotoxicity than

X. Si, Dr. W. Song, S. Yang, L. Ma, C. Yang, Prof. Z. Tang
Key Laboratory of Polymer Ecomaterials
Changchun Institute of Applied Chemistry
Chinese Academy of Sciences, Changchun 130022, P. R. China
E-mail: wtsong@ciac.ac.cn; ztang@ciac.ac.cn
X. Si
University of Science and Technology of China
Hefei 230026, P. R. China
S. Yang
College of Chemistry
Jilin University, Changchun 130012, P. R. China
Dr. W. Song, L. Ma, C. Yang, Prof. Z. Tang
Jilin Biomedical Polymers Engineering Laboratory
Changchun 130022, P. R. China

their non-degradable counterparts after incubation with HeLa cells, indicating that caspase-3 was effectively released into the cells.[21] Ma et al. reported a bioreducible cationic nanogels for antigen delivery. The bioreducible nanogels were constructed though the electrostatic interaction of negatively charged alginate with branched PEI, followed by crosslinking with 3,3'-dithiobis (sulfosuccinimidyl propionate). Ovalbumin (OVA), as a model protein antigen, was loaded into the bioreducible nanogels. The bioreducible nanogels showed high protein loading capacity and good biocompatibility. Subsequently, the immunoregulatory effects were evaluated in vitro and in vivo. The confocal images showed that more OVA were processed by dendritic cells (DCs) than that from the non-reducible nanogels, indicating OVA can release from the nanogels. More antibody production and CD8+ T cell-mediated tumor cell lysis induced by vaccine were observed in vivo. The nanogels have provided a new strategy for protein delivery.[22]

For protein drug carriers, nanostructures formed by spontaneously self-assembly in aqueous solution is preferred. Among them, boronate is a kind of chemical bond which can spontaneously form in aqueous solution by phenyl boronic acid and cis-diol.[23–25] In addition, the boronate is pH and glucose dual-responsive. This specific property made it quite suitable for protein drug delivery, for example, the tumor microenvironment which is known to be acidic and the blood glucose level is extremely high in diabetic patients. Boronic acid can effectively form dynamic covalent structures with sugar, which could respond to hyperglycemia environment and be used as glucose-sensitive linkers.[26–28] Zhao et al. designed a glucose-sensitive micelles based on monomethoxy poly(ethylene glycol)-*b*-poly(L-glutamic acid-*co*-N-3-L-glutamylamidophenylboronic acid) (mPEG-*b*-P(GA-*co*-GPBA). Insulin, a peptide hormone, was loaded into the micelles by hydrophobic interactions. In vitro release profiles revealed the excellent glucose-responsive of boronate. At 1.0 mg mL^{-1} glucose concentration (the preprandial blood glucose level in healthy human body), 29.9% of insulin was released within 14 h; in contrast, 58.5% and 74.8% of insulin were released at 2.0 and 3.0 mg mL^{-1} glucose

solution.[29] Due to these unique properties of boronic acid, polymers containing boronic acid have gained much interest in the areas of detection, materials chemistry, fluorescence imaging, mass spectrometry, and biomedical engineering.[30–33] Diverse nanoplatforms based on boronic acid have been exploited for drug delivery.[34,35]

In this article, a novel nanogel system based on PLG-*g*-mPEG/PBA and dextran was developed aiming at delivery of proteins in a simple and effective way, and keeping the bioactivity of proteins in the process of loading and release. Nanogels were formed by reversible formation of borate between cis-idol in the dextran and the phenyl boronic acid in the PLG-*g*-mPEG/PBA, and protein model drugs were loaded into the nanogel during the gel formation (**Figure 1**). The protein-loaded nanogels were stable under normal physiological environment, while released almost of all the cargos under weak acidic environment and in high glucose condition, detailed physicochemical characteristics, and cytotoxicity study of the nanogel were performed.

2. Experimental Section

2.1. Materials

Hyaluronidase and α-amylase were purchased from Yuan Ye Biotechnology Corporation (Shanghai, P. R. China). N-hydroxysuccinimide (NHS), N-(3-dimethylaminopropyl)-N-ethylcarbodiimide hydrochloride (EDC), and dextran (40 kDa) were purchased from Aladdin Co. Ltd (Shanghai, P. R. China). 3-(4,5-Dimethyl-thiazol-2-yl)-2,5-diphenyl tetrazolium bromide (MTT) was bought from Sigma-Aldrich (Shanghai, P. R. China). Phenyl boronic acid (PBA) was bought from TCI (Shanghai) Development Co., Ltd (Shanghai, P. R. China). γ-Benzyl-L-glutamate-N-carboxyanhydride (BLG-NCA) was purchased from Chengdu Enlai Biological Technology Co., Ltd., China. Other reagents were purchased from the Sinopharm Chemical Reagent Co. Ltd. and used as received.
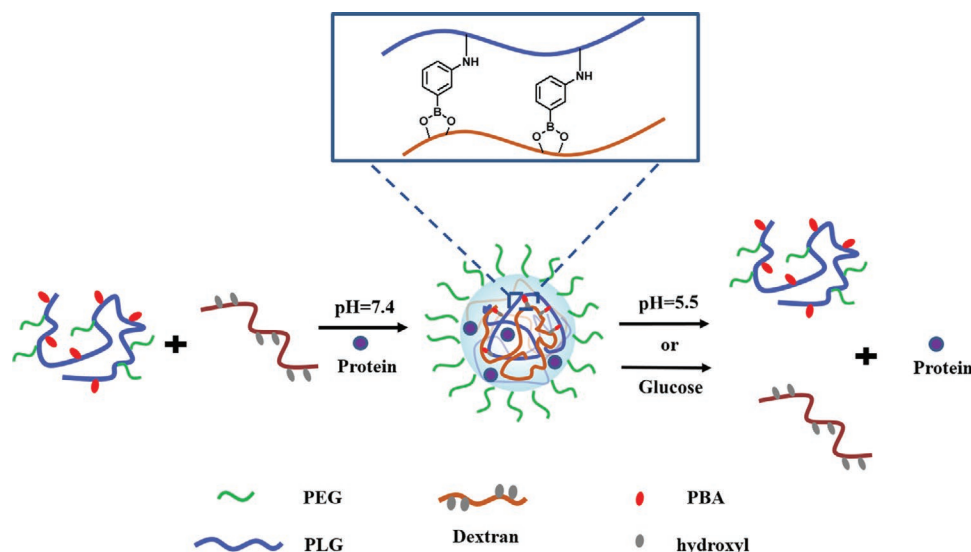

Figure 1. Schematic of pH and glucose dual-responsive nanogels for protein delivery.

ADVANCED
SCIENCE NEWS
www.advancedsciencenews.com

Macromolecular
Bioscience
www.mbs-journal.de

2.2. Methods

^{1}H NMR spectra were recorded on a Bruker AV 300 NMR spectrometer. GPC analyses of PLG-*g*-mPEG and PLG-*g*-mPEG/PBA were equipped with ultra hydrogel linear column and a waters 2414 refractive index detector (eluent: 0.1 M phosphate buffer, pH 7.4; flow rate: 0.5 mL min^{-1}; temperature: 35 °C; standard: poly(ethylene glycol)). Dynamic laser scattering (DLS) measurement was performed on a Wyatt QELS instrument with a vertically polarized He Ne laser (DAWN EOS, Wyatt Technology, USA). The scattering angle was fixed at 90°.

2.3. Synthesis of PLG-*g*-mPEG/PBA

Poly(L-glutamic acid) (PLG) was synthesized through the ring-opening polymerization (ROP) of BLG-NCA and subsequent deprotection. Then mPEG$_{5k}$ was covalently conjugated to PLG to obtain PLG-*g*-mPEGs though the Steglich esterification reaction.[36] Typically, BLG-NCA (40.0 g, 152 mmol) was dissolved in 400 mL anhydrous DMF under a nitrogen atmosphere. Then the initiator, *n*-hexylamine (96.1 mg, 0.951 mmol), was added to the solution. The ring opening polymerization was performed at 25 °C for 3 days before the complex was precipitated into excessive cold ether. Poly(γ-benzyl L-glutamate) (PBLG) was obtained after drying under vacuum overnight. Then the obtained PBLG (20.0 g) was dissolved in 200 mL dichloroacetic acid and then 60 mL of HBr/acetic acid (33 wt%) was added. After being stirred at 30 °C for 1 h, the solution was precipitated into excess ether. After drying under vacuum, the precipitate was redissolved in deionized water, dialyzed (MWCO 3500) against deionized water and freeze-dried to obtain PLG product. 2.0 g of PLG and 6.0 g of dried mPEG$_{5k}$ were dissolved in 40 mL of anhydrous DMF. 49.4 mg (0.404 mmol) of 4-dimethylaminopyridine (DMAP), and 0.62 mL (0.506 g, 4.00 mmol) of diisopropylcarbodiimide (DIC), were added. After stirring at 25 °C for 3 days, the reaction mixture was precipitated into excess ether and washed. After drying under vacuum for overnight, the precipitate was dialyzed with distilled water and freeze-dried to give the PLG-*g*-mPEG product. To synthesize PLG-*g*-mPEG/PBA, PLG-*g*-mPEG (1.50 g, 6.59 mmol −COOH) and anhydrous DMF (50.0 mL) were added in a 100 mL dried flask. After dissolved, EDC (1.18 g, 6.17 mmol) and NHS (0.72 g, 6.17 mmol) were added, followed by activation overnight. Then amino phenyl boronic acid (0.542 g, 0.395 mmol -NH$_2$) was added to the system. Then the above solution was stirred for 48 h at 37 °C oil bath, dialyzed (MWCO 3500) against deionized water for 3 days, filtered through a 0.45 µm pore-sized microporous membrane, and freeze-dried to gain PLG-*g*-mPEG/PBA.

2.4. Preparation and Characterization of Blank and Protein-Loaded Nanogels (Protein-NGs)

PLG-*g*-mPEG/PBA was dissolved in phosphate buffered saline (PBS, 2.0 mL), then dextran with or without protein in PBS was added (3.0 mL) to obtain blank nanogels or protein-NGs. After the above solution was stirred for 6 h, protein-NGs suspension was immediately transferred to a dialysis tube with an MWCO of 100 kDa. Then the tube was centrifuged for 30 min at 5000 rpm. The concentration of residual protein in the tube was measured by a fluorescence spectrometer. The drug-loading content (DLC) and drug-loading efficiency (DLE) of the protein nanogels were calculated using the following formulas:

$$DLC\% = \frac{\text{Amount of protein in protein-NGs}}{\text{Amount of protein-NGs}} \times 100\%$$

$$DLE\% = \frac{\text{Amount of protein in protein-NGs}}{\text{Amount of feeding protein}} \times 100\%$$

2.5. In Vitro Release

To investigate the release behavior of protein-NGs, α-amylase-FITC or hyaluronidase-FITC was prepared according to a previous report.[37] 5.0 mL protein-NGs solution was placed in a dialysis bag (MWCO 100 kDa), then the dialysis bag was incubated in 25.0 mL of phosphate buffered Saline (PBS, pH 7.4/6.8/5.5) or PBS with different concentrations of glucose (1, 3, and 5 mg mL^{-1}) with moderate shaking rate (90 rpm) at 37 °C. At predetermined time points, 3.0 mL of the release solution was withdrawn with same volume fresh PBS supplemented. The concentration of protein in the released media was tested by fluorescence spectrometer.

2.6. Circular Dichroism Test

The secondary structure of the released protein was characterized by circular dichroism (CD) spectroscopy (Biologic MOS-450 CD spectrophotometer) at 25 °C with a cell length of 0.1 cm. For samples were scanned from 180 to 260 nm with the scanning speed of 1 nm per 10 s. All CD data are expressed as residue ellipticity. The peaks at 208 and 222 nm indicate the alpha-helix, the peak at 218 nm indicates the beta-strand of protein.

2.7. The Activity of Released α-Amylase

The activity of released α-amylase was measured by 3,5-dinitrosalicylic acid (DNS) method.[38] One milliliter of released α-amylase solution was added to 2.0 mL phosphate buffer saline (pH 7.4), containing 10 mg mL^{-1} starch. After the solution was well mixed, it was immediately incubated in 37 °C water bath, then 1.0 mL DNS solution was added. The mixed solution was placed in a boiling water bath for 5 min, then cooled in running water for 5 min. The solution was diluted into 15 mL with deionized water. The absorbance was measured at 520 nm for the DNS procedure.

DNS reagent was obtained by the following method. Sodium hydroxide (1.6 g) and DNS (1.0 g) was dissolved in distilled water (100 mL). Then potassium sodium tartrate tetrahydrate (3.0 g) was added. After stored for 7–10 days in dark, the obtained solution can be used for quantification of α-amylase.

2.8. Cell Culture

The mouse breast cancer cell line, 4T1 and CT26, were obtained from Shanghai Bogoo Biotechnology Co., Ltd. Cells were cultured at 37 °C in a 5% CO_2 atmosphere in Dulbecco's modified Eagle's medium (DMEM, Gibco) with high glucose containing 10% fetal bovine serum (FBS), supplemented with 1% penicillin and 1% streptomycin.

2.9. Cellular Uptake

α-Amylase was labelled by Cy5 to obtain α-amylase-Cy5 for the CLSM assay. 10^5 CT26 cells per well were seeded onto glass coverslips placed in the 6-wells plate and incubated overnight for cell adherence culture with 2 mL DMEM, then replaced with fresh DMEM with α-amylase-Cy5 or α-amylase-Cy5 loaded nanogels (at a final α-amylase-Cy5 concentration of 4 mg mL^{-1}). After 6 h, the cells were washed with 3 mL PBS for three times and fixed with 4% formaldehyde for 20 min at room temperature, followed by washing the residual formaldehyde with 3 mL PBS for three times. According to the manufacturer's instructions, the cell nuclei were stained with DAPI. The coverslips were placed onto glass microscope slides and fixed with nail polish, and the cellular uptake of α-amylase-Cy5 was visualized using a CLSM (Carl Zeiss LSM 700).

2.10. Cellular Cytotoxicity Assay In Vitro

To assess the biocompatibility of PLG-*g*-mPEG/PBA and dextran, 4T1 cell proliferations in vitro were evaluated after 48 or 72 h incubation with blank nanogels. The cells were plated in 96-well culture plates at a density of 7000 cells per well and incubated overnight for cell adherence culture, then replaced with 200 μL fresh DMEM with different concentration of PLG-*g*-mPEG/PBA and dextran. After 24 or 48 h incubation, 20 μL of MTT stock (1 mg mL^{-1} in sterile PBS) were added into each well. Incubated for another 4 h, the supernatant was removed and 150 μL DMSO was added. The absorbance of the solution was measured on a Bio-Rad 680 microplate reader at 490 nm. The relative cell viability (%) was calculated by the following formulas:

$$\text{Cell } viability\left(\%\right) = \left(A_{\text{experimental}} / A_{\text{control}}\right) \times 100$$

$A_{\text{experimental}}$ and A_{control} represent absorbance of the experimental well and control well, respectively. Data are presented as average ± SD ($n = 3$).

3. Results and Discussion

3.1. Characterization of PLG-*g*-mPEG/PBA

The ^{1}H NMR spectrum of PLG-*g*-mPEG/PBA is shown in **Figure 2**. The signals of C_6H_5-(d/e/g/f) in phenyl boronic acid unit are at δ 7.02–7.60 ppm. The signal at δ 11.5 ppm is the
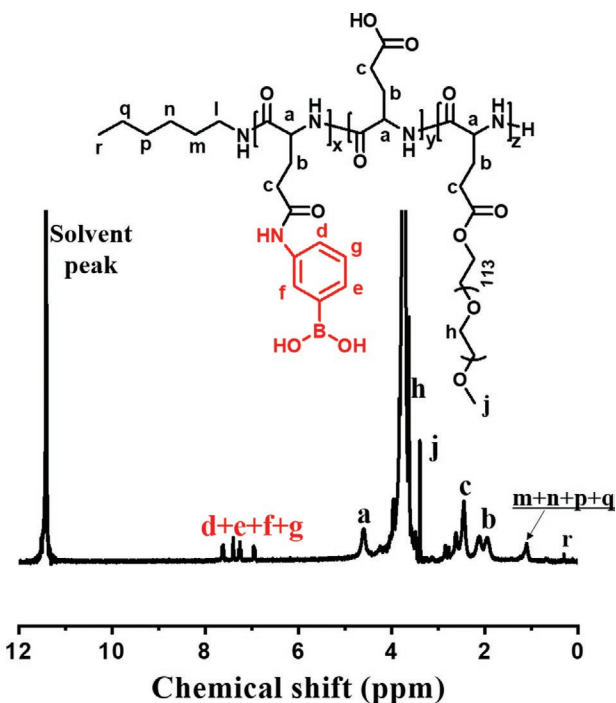

Figure 2. The ^{1}H NMR spectrum of PLG-*g*-mPEG/PBA in TFA-*d*.

peak of solvent TFA. The signal δ 3.82 ppm is -CH_2CH_2O- (h) in PEG units. The signal δ 3.46 ppm is CH_3O- (j) in PEG. The signals δ 4.51 ppm, δ 2.38–2.65 ppm and δ 1.81–2.22 ppm are -CH<(a), -CH_2CO- (c) and –$CHCH_2$- (b) in PLG units, respectively. Though the ratio of C_6H_5- (d/e/f/g) and -CH_2CH_2O- (h), the average number of PBA conjugated to PLG chain is 25. GPC analyses (**Figure 3**) showed the number average molecule weight (M_n) of PLG-*g*-mPEG/PBA and PLG-*g*-mPEG are 64.1 × 10^3 Da and 68.4 × 10^3 Da, while the poly dispersity index (PDI, M_w/M_n) are 1.59 and 1.21, respectively. All these results confirm the successful conjugation of phenyl boronic acid groups to PLG-*g*-mPEG.
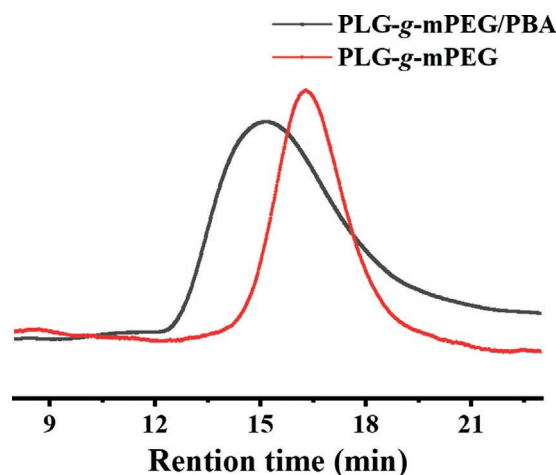

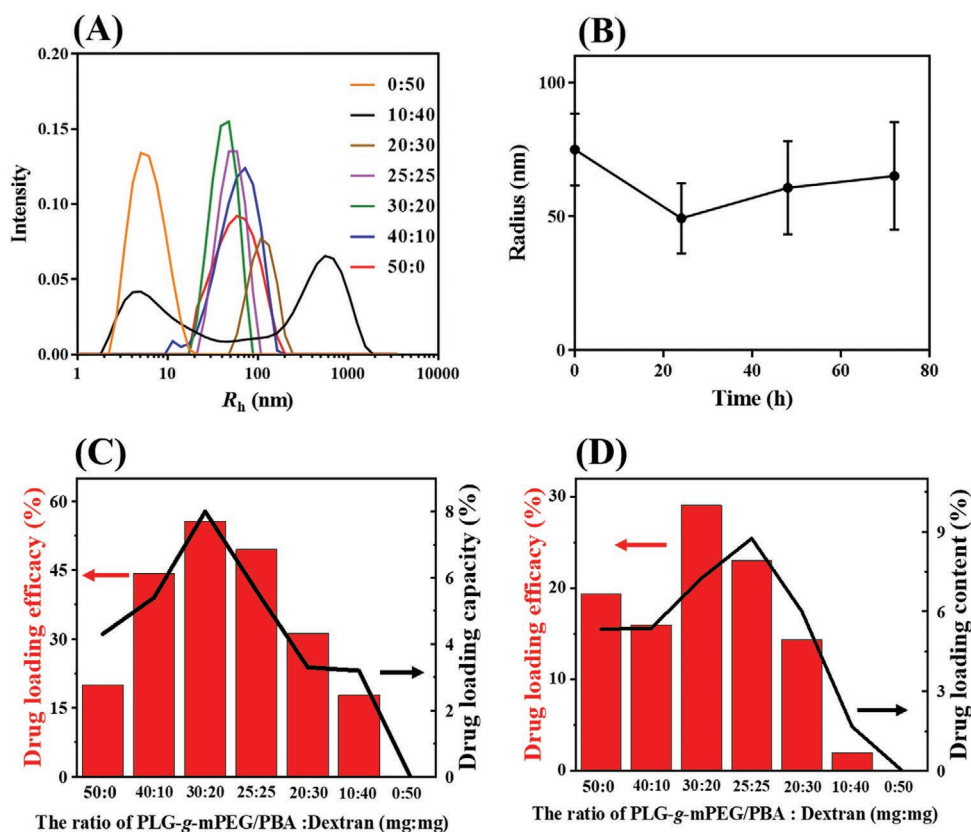**Figure 3.** GPC traces of PLG-*g*-mPEG and PLG-*g*-mPEG/PBA in DMF.

Figure 4. A) Hydrodynamic radius distribution of nanogels in different ratios. The hydrodynamic radius was calculated based on peak means. B) Sizes and intensities of nanogels in PBS at 37 °C ($n = 3$). C) Influence of mass proportion of PLG-*g*-mPEG/PBA and dextran on the DLE and DLC of α-amylase and D) Influence of mass proportion of PLG-*g*-mPEG/PBA and dextran on the DLE and DLC of hyaluronidase.

3.2. Preparation and Characterization of Blank Nanogels and Protein-Loaded Nanogels

Different ratios of PLG-*g*-mPEG/PBA and dextran, from 50:0 to 0:50 (w/w), were applied in preparing the nanogels. As shown in **Figure 4**A, when the weight ratio of PLG-*g*-mPEG/PBA: dextran was 50:0, there was only PLG-*g*-mPEG/PBA, the hydrodynamic radius was 82 ± 61 nm. With the addition of more dextran, smaller hydrophobic core was formed due to the crosslinking between PBA and dextran, and the radius decreased. When the ratio of PLG-*g*-mPEG/PBA: dextran was 30:20, the radius of the formed nanogel was 44 ± 27 nm. The crosslinking density was the highest and the size of nanogels was the smallest. Continued addition of dextran resulted in reduced cross-linking density and increased nanogel sizes. Therefore, we used the ratio of 30:20 in the following study. The stability of α-amylase-loaded nanogels in PBS was assessed by monitoring changes in the size of the nanogels. At determined time intervals, the solution of α-amylase-loaded nanogels was taken out, and the nanogel sizes were measured by DLS. As shown in Figure 4B, the radius of nanogels kept constant at 65 ± 22 nm within 72 h, with no significant size or intensity changes happening, suggesting the stability of nanogels. The zeta potential of blank nanogels was −40 ± 4 mv.

Inspired by the appropriate size and stability, α-amylase and hyaluronidase as model proteins, were loaded to form protein-loaded nanogels. Various PLG-*g*-mPEG/PBA and dextran ratios were tested for protein-loading efficiency. When the ratio of PLG-*g*-mPEG/PBA: dextran was 30:20, the DLC and DLE of α-amylase could reach the most of 8.0% and 67.1% (Figure 4C), and the DLC and DLE of hyaluronidase is 8.8% and 23.0% (Figure 4D). The results were in good agreement with the change of radius, indicating that the weight ratio of PLG-*g*-mPEG/PBA: dextran at 30:20 was the condition for obtaining nanogels with smallest size and highest crosslinking density. At this condition, intact nanostructures were formed and high loading capacity was obtained.

The size and morphology of α-amylase-loaded nanogels were further characterized by TEM. When the weight ratio of PLG-*g*-mPEG/PBA: dextran was 30:20, the radius of blank nanogels was 67 ± 23 nm, and the blank nanogels had uniform sphere morphology (**Figure 5**A). The radius of α-amylase-loaded nanogels was 85 ± 35 nm (Figure 5B). After incubation in pH 5.5 buffer for 24 h, most of the nanogels were disassembled (Figure 5C).

In order to get the maximum α-amylase loading amount of the nanogel, different doses of α-amylase have been fed for nanogels which were composed of PLG-*g*-mPEG/PBA (30.0 mg) and dextran (20.0 mg). As shown in **Table 1**, when the α-amylase was increased from 2.50 to 10.0 mg, the amount of loaded α-amylase was increased from 2.11 to 4.10 mg. Further increase of the α-amylase could not result in more α-amylase
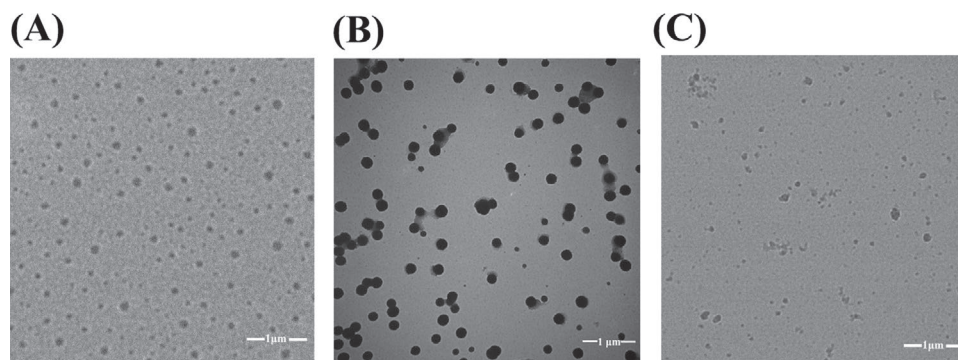
(A) (B) (C)

Figure 5. A) The TEM image of blank nanogels The scale bar is 1 µm. B)The TEM image of α-amylase-loaded nanogels in PBS at pH 7.4. The scale bar is 1 µm. C)The TEM image of released α-amylase-loaded nanogels at pH 5.5. The scale bar is 1 µm.

Table 1. Drug-loading efficiency test results of α-amylase in nanogel when the ratio is 30/20.

PLG-g-mPEG/PBA [mg]	Dextran [mg]	Feed α-amylase [mg]	Loaded α-amylase [mg]	DLE [%]
30.0	20.0	2.50	2.11	84.4
30.0	20.0	5.00	3.08	61.6
30.0	20.0	10.0	4.10	44.0
30.0	20.0	15.0	4.13	27.5
30.0	20.0	20.0	4.14	20.7
30.0	20.0	25.0	4.67	18.7

loading. Therefore, we used a feeding amount of 10 mg for further studies.

3.3. Release Behavior of Nanogels and CD Spectrum of the Released Protein

In view the fact that the microenvironment of solid tumors is acidic, and the the blood level of diabetics is high. The blood pH is 7.4, while pH of extracellular fluid of solid tumor is 6.5–6.8. Intracellular fluid pH can reach 5.0–5.5.[39] The preprandial blood glucose concentration in the healthy human body is about 1.0 mg mL^{-1}, and the prandial blood glucose concentration in the healthy human body is below 1.5 mg mL^{-1}, while the prandial blood glucose level in diabetics body is above 2.0–4.0 mg mL^{-1}. So the release behavior in vitro was studied in PBS at different pH (pH 5.5, 6.8, or 7.4) and PBS (pH 7.4) with different glucose concentrations (0, 1, 3, 5 mg mL^{-1}). As shown in **Figure 6**A, the accumulated α-amylase release at pH 5.5, 6.8, and 7.4 were 86.2%, 38.3%, and 18.9% in 72 h, respectively. The cargos were more effectively released from the nanogels in the acidic environment, suggesting potential as the carrier of anti-tumor protein drug delivery. When different concentrations of glucose were added into the PBS (pH 7.4) to simulate the blood environment of healthy and diabetic individuals, 40.2%, 72.8%, 81.5% of α-amylase were released within 72 h at the glucose concentration of 1, 3, and 5 mg mL^{-1}, respectively (Figure 6B). The glucose-responsive release

property of nanogels may suggest potential for diabetes protein drug delivery. Then the released α-amylase at different conditions were characterized by CD spectroscopy (Figure 6C,D). The peaks at 208 and 222 nm showed the alpha-helix, the peak at 218 nm showed the beta-strand of protein.[40] The peaks of released α-amylase were same with pure α-amylase, proved that nanogels can effectively maintain the secondary structure of protein. To further verify the loading and release capacity of nanogels, hyaluronidase, a protein can catalyze the degradation of hyaluronic acid (HA) and enhance the permeability of solid tumor, was loaded to obtain hyaluronidase-loaded nanogels.[41] Similarly, approximately 82.7%, 57.4%, and 41.1% of total hyaluronidase were released from the protein nanogels within 72 h at pH 5.5, 6.5, and 7.4 (**Figure 7**A), revealing pH responsiveness of nanogels. And the CD of released hyaluronidase was same with pure hyaluronidase, suggesting that the activity of protein was kept during the loading and release process (Figure 7B).

3.4. The Residual Activity of Released Protein

The activity of released α-amylase was measured by the 3,5-dinitrosalicylic acid (DNS) method. 3,5-Dinitrosalicylic acid (DNS) is an aromatic compound that reacts with reducing sugars to form 3-amino-5-nitrosalicylic acid, which has strong absorbance at 540 nm. It was mainly used for quantification of reducing sugar. Starch can be reduced to reducing sugar by α-amylase, so DNS method can also be widely used for quantification of α-amylase activity. As shown in **Figure 8**, when the accumulated release of α-amylase reached 86.2% in PBS (pH 5.5), the activity of α-amylase was remained about 95.0%. Most activity of α-amylase remained, proving the nanogels were potential carriers of load and release protein.

3.5. Cellular Uptake

The cellular uptake of α-amylase-Cy5 or α-amylase-Cy5 loaded nanogels were investigated by CLSM after incubation with CT26 cells at 37 °C for 6 h. Cell nucleus were stained blue with DAPI. Red fluorescence imaging was carried out to visualize
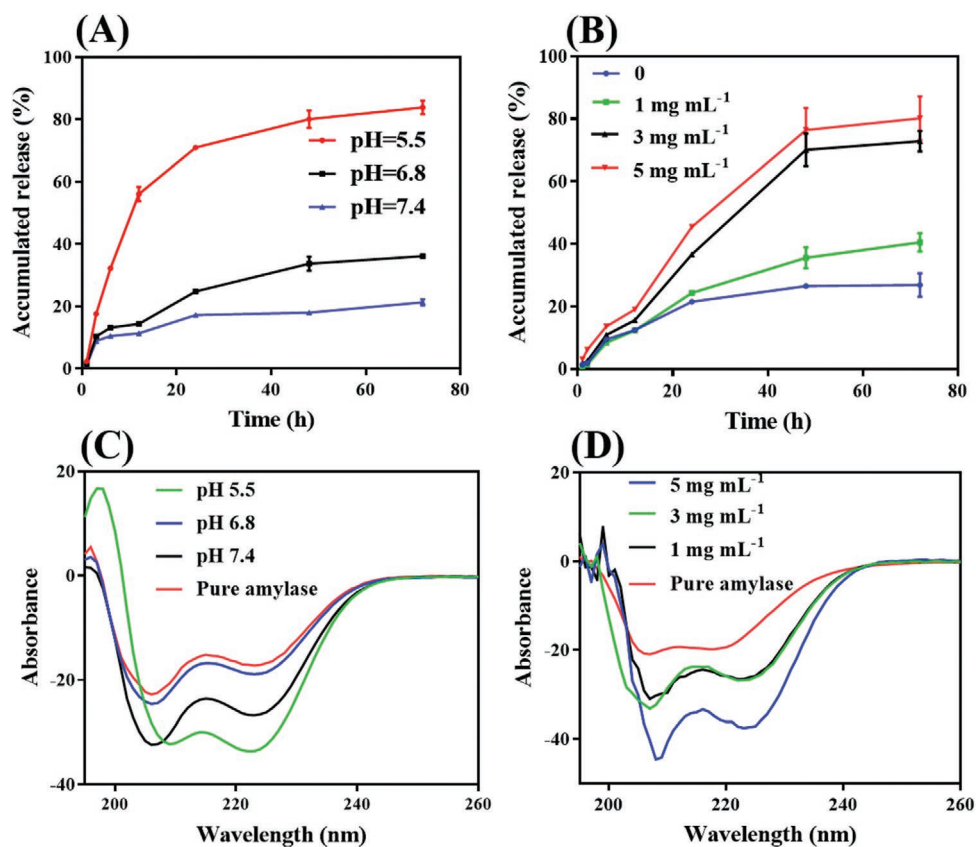
ADVANCED
SCIENCE NEWS
www.advancedsciencenews.com

Macromolecular
Bioscience
www.mbs-journal.de

Figure 6. A) In vitro pH responsive release profiles of α-amylase-loaded nanogels. B) In vitro glucose-responsive release profiles of α-amylase-loaded nanogels at different glucose concentration (5, 3, 1 mg mL^{-1}) in PBS (pH 7.4). C) The CD of the released α-amylase at different pH and pure α-amylase. D) The CD of the released α-amylase at different glucose concentrations and pure α-amylase. Each datum represented the average of three independent determinations.

α-amylase-Cy5. As shown in **Figure 9**, α-amylase loaded in nanogels was internalized into CT26 cells efficiently, while no pure α-amylase detected intracellularly at the same condition, revealing that α-amylase-Cy5 could be internalized after encapsulating with nanogels.

3.6. Biocompatibility of Nanogels

In this work, the cytotoxicity of PLG-*g*-mPEG/PBA and dextran to murine breast cancer 4T1 cells was evaluated using the MTT assay. 4T1 cells were treated with blank nanogels at
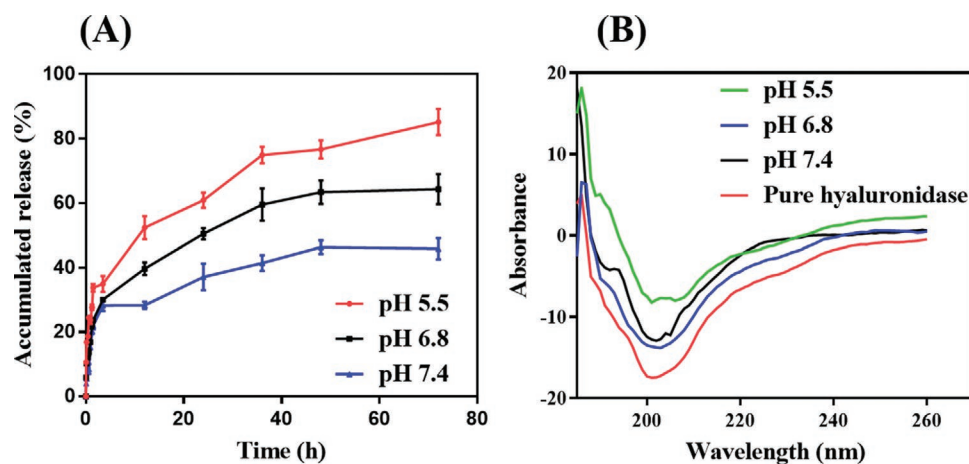

Figure 7. A) In vitro release profiles of hyaluronidase-loaded nanogels. B) The CD of the hyaluronidase released at different pH conditions and pure hyaluronidase.
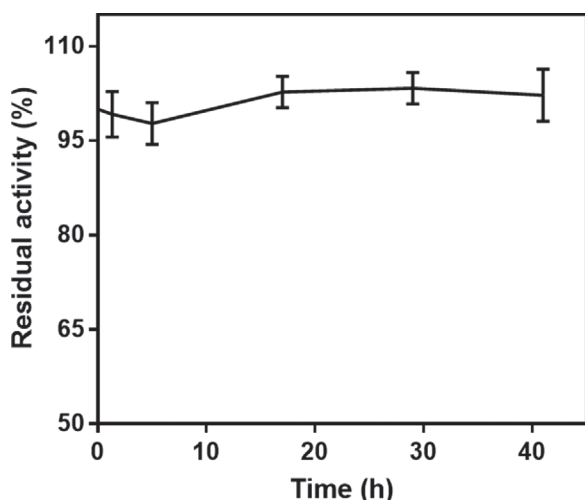
Figure 8. The residual activity of α-amylase released from PBS at pH 5.5.
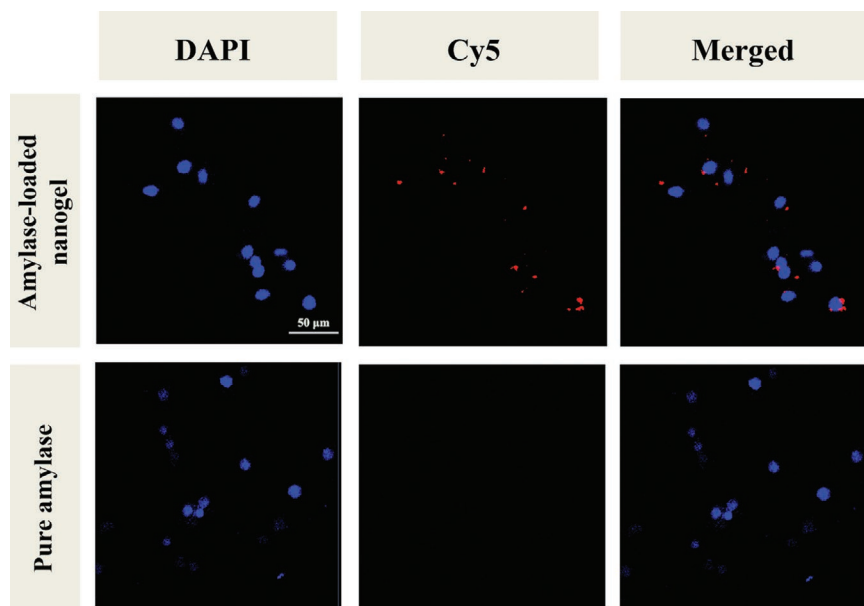
the predetermined concentrations for 24 and 48 h. As shown in **Figure 10**, the viability of 4T1 cells treated with blank nanogels was around 91–110% at all test concentrations up to 1 mg mL^{-1}, indicating its low toxicity and good compatibility.

4. Conclusions

In this article, we have designed a pH and glucose dual-responsive nanogel. Nanogels are formed by crosslinking between by dextran and PLG-g-mPEG/PBA. PBA can effectively form boronate bond with cis-diol in aqueous solution free of organic solution, which is optimal for loading protein. The size of nanogels was closely related to the content ratio. When the ratio of PLG-g-mPEG/PBA: dextran was 30:20, the radius of nanogels attained the minimum of 43.7 nm, and the nanogels had the best loading capacity in this ratio. α-Amylase and hyaluronidase, as the model proteins, were loaded into the nanogels and the release could be triggered by weak acidic environment or high glucose level. Furthermore, the protein released from the nanogels maintains its secondary structure and activity. The MTT result shows the excellent biocompatibility of nanogels. In brief, the nanogel has offered a new strategy for protein delivery.

Figure 9. CLSM images of CT26 cells after incubation with α-amylase-loaded nanogels or pure amylase for 6 h. α-amylase was labeled with Cy5. Scale bar: 50 µm.

Conflict of Interest

The authors declare no conflict of interest.
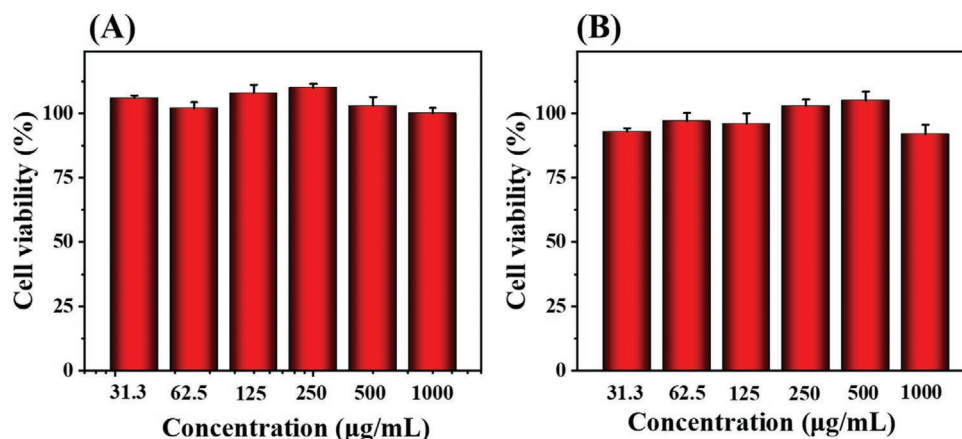
Figure 10. In vitro cytotoxicity of blank nanogels to 4T1 cells at A) 24 h and B) 48 h.

[1] Y. Lu, W. Sun, Z. Gu, *J. Controlled Release* **2014**, *194*, 1.

[2] H. Patterson, R. Nibbs, I. McInnes, S. Siebert, *Clin. Exp. Immunol.* **2014**, *176*, 1.

[3] M. Komori, P. Kosa, J. Stein, V. Zhao, A. Blake, J. Cherup, J. Sheridan, T. Wu, B. Bielekova, *Ann. Clin. Trans. Neurol.* **2017**, *4*, 478.

[4] W. Song, K. Tiruthani, Y. Wang, L. Shen, M. Hu, O. Dorosheva, K. Qiu, K. A. Kinghorn, R. Liu, L. Huang, *Adv. Mater.* **2018**, *30*, 1805007.

[5] R. Kumar, T. A. Bhat, E. M. Walsh, A. K. Chaudhary, J. O'Malley, J. S. Rhim, J. Wang, C. D. Morrison, K. Attwood, W. Bshara, J. L. Mohler, N. Yadav, D. Chandra, *Cancer Res.* **2019**, *79*, 1353.

[6] Z. Zhao, X. Yao, Z. Zhang, L. Chen, C. He, X. Chen, *Macromol. Biosci.* **2014**, *14*, 1609.

[7] Y. Chen, W. Song, L. Shen, N. Qiu, M. Hu, Y. Liu, Q. Liu, L. Huang, *ACS Nano* **2019**, *13*, 1751.

[8] W. Song, L. Shen, Y. Wang, Q. Liu, T. J. Goodwin, J. Li, O. Dorosheva, T. Liu, R. Liu, L. Huang, *Nat. Commun.* **2018**, *9*, 2237.

[9] J. C. Campos, J. D. Cunha, D. C. Ferreira, S. Reis, P. J. Costa, *Eur. J. Pharm. Biopharm.* **2018**, *128*, 131.

[10] M. Kristensen, D. Birch, H. Morck Nielsen, *Int. J. Mol. Sci.* **2016**, *17*, 185.

[11] I. El-Sherbiny, I. Khalil, I. Ali, M. Yacoub, *Drug Dev. Ind. Pharm.* **2017**, *43*, 1567.

[12] M. R. Villegas, A. Baeza, M. Vallet-Regi, *Molecules* **2018**, *23*, 1008.

[13] H. He, J. Ye, Y. Wang, Q. Liu, H. S. Chung, Y. M. Kwon, M. C. Shin, K. Lee, V. C. Yang, *J. Controlled Release* **2014**, *176*, 123.

[14] Z. Zhang, W. Shen, J. Ling, Y. Yan, J. Hu, Y. Cheng, *Nat. Commun.* **2018**, *9*, 1377.

[15] J. Wu, N. Kamaly, J. Shi, L. Zhao, Z. Xiao, G. Hollett, R. John, S. Ray, X. Xu, X. Zhang, P. W. Kantoff, O. C. Farokhzad, *Angew. Chem., Int. Ed.* **2014**, *53*, 8975.

[16] W. Song, S. N. Musetti, L. Huang, *Biomaterials* **2017**, *148*, 16.

[17] G. Soni, K. S. Yadav, *Saudi Pharmaceut. J.* **2016**, *24*, 133.

[18] W. Song, M. Das, Y. Xu, X. Si, Y. Zhang, Z. Tang, X. Chen, *Mater. Today Nano* **2019**, *5*, 100029.

[19] B. Li, Q. Xu, X. Li, P. Zhang, X. Zhao, Y. Wang, *Carbohydr. Polym.* **2019**, *203*, 378.

[20] Y. Q. Xie, H. Arik, L. Wei, Y. Zheng, H. Suh, D. J. Irvine, L. Tang, *Biomater. Sci.* **2019**, *7*, 1345.

[21] D. Li, C. F. van Nostrum, E. Mastrobattista, T. Vermonden, W. E. Hennink, *J. Controlled Release* **2017**, *259*, 16.

[22] D. Li, N. Kordalivand, M. F. Fransen, F. Ossendorp, K. Raemdonck, T. Vermonden, W. E. Hennink, C. F. van Nostrum, *Adv. Funct. Mater.* **2015**, *25*, 2993.

[23] H. Gaballa, J. Shang, S. Meier, P. Theato, *J. Polym. Sci., Part A: Polym. Chem.* **2019**, *57*, 422.

[24] S. Y. Lee, H. Lee, I. In, S. Y. Park, *Eur. Polym. J.* **2014**, *57*, 1.

[25] B. Yang, Y. Lv, J. Y. Zhu, Y. T. Han, H. Z. Jia, W. H. Chen, J. Feng, X. Z. Zhang, R. X. Zhuo, *Acta Biomater.* **2014**, *10*, 3686.

[26] X.-Q. Zhao, T.-X. Wang, W. Liu, C.-D. Wang, D. Wang, T. Shang, L.-H. Shen, L. Ren, *J. Mater. Chem.* **2011**, *21*, 7240.

[27] V. L. Dhadge, A. Hussain, A. M. Azevedo, R. Aires-Barros, A. C. Roque, *J. R. Soc., Interface* **2013**, *11*, 20130875.

[28] Z. Zhao, X. Yao, Z. Zhang, L. Chen, C. He, X. Chen, *Macromol. Biosci.* **2014**, *14*, 1609.

[29] L. Zhao, J. Ding, C. Xiao, P. He, Z. Tang, X. Pang, X. Zhuang, X. Chen, *J. Mater. Chem.* **2012**, *22*, 12319.

[30] Z. Wu, S. Zhang, X. Zhang, S. Shu, T. Chu, D. Yu, *J. Pharm. Sci.* **2011**, *100*, 2278.

[31] T. Nochi, H. Yuki, H. Takahashi, S. Sawada, M. Mejima, T. Kohda, Y. Takahashi, H. Tsukada, S. Kozaki, K. Akiyoshi, H. Kiyono, *Nat. Mater.* **2010**, *9*, 572.

[32] W. Xu, J. Ding, L. Li, C. Xiao, X. Zhuang, X. Chen, *Chem. Commun.* **2015**, *51*, 6812.

[33] Z. Liu, N. Shen, Z. Tang, D. Zhang, L. Ma, C. Yang, X. Chen, *Biomater. Sci.* **2019**, *7*, 2803.

[34] T. Aikawa, T. Konno, M. Takai, K. Ishihara, *Langmuir* **2012**, *28*, 2145.

[35] S. Lv, Y. Wu, K. Cai, H. He, Y. Li, M. Lan, X. Chen, J. Cheng, L. Yin, *J. Am. Chem. Soc.* **2018**, *140*, 1235.

[36] J. Yan, D. Zhang, H. Yu, L. Ma, M. Deng, Z. Tang, X. Zhang, *J. Biomater. Sci., Polym. Ed.* **2017**, *28*, 394.

[37] Q. Chen, C. Wang, X. Zhang, G. Chen, Q. Hu, H. Li, J. Wang, D. Wen, Y. Zhang, Y. Lu, G. Yang, C. Jiang, J. Wang, G. Dotti, Z. Gu, *Nat. Nanotechnol.* **2019**, *14*, 89.

[38] A. Machado, R. Maneiras, A. A. Bordalo, R. B. R. Mesquita, *Talanta* **2018**, *186*, 192.

[39] M. Upreti, A. Jyoti, P. Sethi, *Transl. Cancer Res.* **2013**, *2*, 309.

[40] W. Z. Yang, T. P. Ko, L. Corselli, R. C. Johnson, H. S. Yuan, *Protein Sci.* **1998**, *7*, 1875.

[41] X. W. Guan, J. Chen, Y. Y. Hu, L. Lin, P. J. Sun, H. Tian, X. S. Chen, *Biomaterials* **2018**, *171*, 198.